Inorg. Chem. **2005**, *44*, 8285–8292

Synthesis, Structures, and Magnetic Properties of Heteronuclear Cu(II)–Ln(III) (Ln = La, Gd, or Tb) Complexes

Feng He,[†,‡] Ming-Liang Tong,[†] and Xiao-Ming Chen*[,†]

State Key Laboratory of Optoelectronic Materials and Technologies, School of Chemistry and Chemical Engineering, and School of Pharmaceutical Science, Sun Yat-Sen University, Guangzhou 510275, P. R. China

Received May 7, 2005

Facile one-pot reactions led to the formations of dinuclear $[CuLn(hmp)_2(NO_3)_3(H_2O)_2]$ (Ln = Tb (**1**·Tb), Gd (**1**·Gd), or La (**1**·La)), and trinuclear $[Cu_2Ln(mmi)_4(NO_3)(H_2O)_2](ClO_4)(NO_3)\cdot 2H_2O$ (Ln = Tb (**2**·Tb) or Gd (**2**·Gd)) and $[Cu_2La(mmi)_4(NO_3)_2(H_2O)](ClO_4)\cdot 2H_2O$ (**2**·La) with polydentate ligands 2-(hydroxymethyl)-pyridine and 2-hydroxymethyl-1-methyl-imidazole. In these complexes, each pair of Cu(II) and Ln(III) ions is linked by a double μ-alkoxo bridge. The temperature dependences of the magnetic susceptibilities of **1** and **2** were investigated in the range of 2–300 K. The dinuclear and trinuclear Cu–Gd complexes exhibit ferromagnetic interaction. The coupling constant *J* values in the heterodinuclear Cu–Gd complexes are correlated to values of the dihedral angles α between the two O–Cu–O and O–Gd–O fragments of the bridging CuO_2Gd networks, with the largest *J* value associated with the smallest α value. The occurrence of a ferromagnetic interaction between Cu^{II} and Gd^{III} ions of the trinuclear entity is supported by the field dependence of the magnetization. The field dependence of the magnetization at 2 K of **1**·Gd and **2**·Gd confirms the nature of the ground state and of the Cu^{II}–Gd^{III} interaction, while alternating current susceptibility measurements demonstrates out-of-phase ac susceptibility signals of **1**·Tb, which is the molecule-based magnetic material of the smallest nuclearity which exhibits frequency-dependent behavior within the 3d–4f mixed-metal systems.

The design and synthesis of new molecule-based magnetic materials have become one of the most active areas in the molecular material chemistry field,[1] where metal complexes exhibiting versatile magnetic behaviors, such as single molecule magnets (SMM), have attracted special attention over the past decade, and the molecular-based magnetic materials consisting of d-transition metal ions have been widely investigated.[2−7] In contrast, the magnetochemistry of d−f heterometallatic complexes is not well developed in this field. To date, a number of homonuclear clusters have been observed displaying frequency-dependent behavior,[5−7] in which one dinuclear complex[5c] was reported. Recently, only a few of the 3d−4f complexes[8,9] within mixed-metal systems[8−10] exhibited frequency-dependent out-of-phase (χ_M'') signals.

* E-mail: cescxm@zsu.edu.cn. Fax: Int. code +86 20 8411-2245.
† School of Chemistry and Chemical Engineering.
‡ School of Pharmaceutical Science.

(1) (a) Wernsdorfer, W.; Aliaga-Alcalde, N.; Hendrickson, D. N.; Christou, G. *Nature* **2002**, *416*, 406−409. (b) Barco, E. D.; Kent, A. D.; Rumberger, E. M.; Hendrickson D. N.; Christou, G. *Phys. Rev. Lett.* **2003**, *91*, 047203.
(2) (a) Wernsdorfer, W.; Sessoli, R. *Science* **1999**, *284*, 133−135. (b) Leuenberger, M. N.; Loss, D. *Nature* **2001**, *410*, 789−793.
(3) For review, see: Gatteschi, D.; Sessoli, R. *Angew. Chem., Int. Ed.* **2003**, *42*, 268−297.
(4) (a) Caneschi, A.; Gatteschi, D.; Sessoli, R.; Barra, A. L.; Brunel, L. C.; Guillot, M. *J. Am. Chem. Soc.* **1991**, *113*, 5873−5874. (b) Sessoli, R.; Gatteschi, D.; Caneschi, A.; Novak, M. A. *Nature* **1993**, *365*, 141−143.
(5) (a) Tasiopoulos, A. J.; Vinslava, A.; Wernsdorfer, W.; Abboud, K. A.; Christou, G. *Angew. Chem., Int. Ed.* **2004**, *43*, 2117−2121. (b) Berlinguette, C. P.; Vaughn, D.; Canada-Vilalta, C.; Galán-Mascaros, J. R.; Dunbar, K. R. *Angew. Chem., Int. Ed.* **2003**, *43*, 1523−1526. (c) Miyasaka, H.; Clérac, R.; Wernsdorfer, W.; Lecren, L.; Bonhomme, C.; Sugiura, K.-i.; Yamashita, M. *Angew. Chem., Int. Ed.* **2004**, *43*, 2801−2805.
(6) (a) Andres, H.; Basler, R.; Blake, A. J.; Cadiou, C.; Chaboussant, G.; Grant, C. M.; Güdel, H.-U.; Murrie, M.; Parsons, S.; Paulsen, C.; Semadini, F.; Villar, V.; Wernsdorfer, W.; Winpenny, R. E. P. *Chem. Eur. J.* **2002**, *8*, 4867−4876. (b) Murrie, M.; Teat, S. J.; Stœckli-Evans, H.; Güdel, H. U. *Angew. Chem., Int. Ed.* **2003**, *42*, 4653−4656. (c) Boskovic, C.; Brechin, E. K.; Streib, W. E.; Folting, K.; Bollinger, J. C.; Hendrickson, D. N.; Christou, G. *J. Am. Chem. Soc.* **2002**, *124*, 3725−3736.
(7) (a) Boudalis, A. K.; Donnadieu, B.; Nastopoulos, V.; Clemente-Juan, J. M.; Mari, A.; Sanakis, Y.; Tuchagues, J.-P.; Perlepes, S. P. *Angew. Chem., Int. Ed.* **2004**, *43*, 2266−2270. (b) Miyasaka, H.; Nakata, K.; Sugiura, K.-i.; Yamashita, M.; Clérac, R. *Angew. Chem., Int. Ed.* **2004**, *43*, 707−711. (c) Lecren, L.; Li, Y.-G.; Wernsdorfer, W.; Roubeau, O.; Miyasaka, H.; Clérac, R. *Inorg. Chem. Commun.* **2005**, *8*, 626−630.

10.1021/ic0507159 CCC: $30.25
Published on Web 10/11/2005

Meanwhile, in the growing field of heterometallic 3d−4f complexes, the magnetic coupling between 3d and 4f ions is, so far, less understood. For example, the intramolecular interaction between Cu^{II} and Gd^{III} has been found to be ferromagnetic in most cases.[11−14] However, there are also a few examples in the recent literature that show weak antiferromagnetic behaviors do exist.[15] The results from these studies[16,17] show a need for a clear explanation on the nature of the magnetic coupling between 3d and 4f ions.

In the course of our investigations into 3d−4f complexes, we have reported a series of Cu^{II}−Ln^{III} complexes with carboxylate and hydroxide bridges over the past decade.[18,19] Such 3d−4f complexes could yield interesting magnetic properties due to the large uniaxial anisotropy inherent to these ions,[8] which is a necessary condition to generate SMMs. We recently used the chelating, pyridine-based ligand 2-(hydroxymethyl)-pyridine (Hhmp) and its imidazole-based analogue 2-hydroxymethyl-1-methyl-imidazole (Hmmi) (Chart 1) as bridging ligands. Hhmp has already proven very useful in the synthesis of Mn clusters as SMMs,[7b,c] while Hmmi

Chart 1

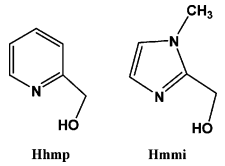

Hhmp Hmmi

was synthesized previously by our group.[20] Under similar reaction conditions, we isolated dinuclear $[CuLn(hmp)_2(NO_3)_3(H_2O)_2]$ (Ln = Tb (**1**·Tb), Gd (**1**·Gd), or La (**1**·La)), and trinuclear $[Cu_2Tb(mmi)_4(NO_3)(H_2O)_2](ClO_4)(NO_3)\cdot 2H_2O$ (Ln = Tb (**2**·Tb) or Gd (**2**·Gd)) and $[Cu_2La(mmi)_4(NO_3)_2(H_2O)](ClO_4)\cdot 2H_2O$ (**2**·La) by facile one-pot reactions and the synthesis, crystal structures, and magnetic properties are described herein.

Experimental Section

All chemicals were purchased from commercial vendors and used without further purification. The C, H, and N microanalyses were carried out with a Perkin-Elmer 240Q elemental analyzer. FT−IR spectra were recorded from KBr pellets in the range of 4000−400 cm^{-1} on a Nicolet 5DX spectrometer. The variable-temperature magnetic-susceptibility data were measured with a Quantum Design MPMS7 SQUID magnetometer. Magnetic measurements were performed on samples of crushed single crystals in the 2−300 K range. The magnetic susceptibility (χ_M) has been measured in a 1 KOe dc field and in a 3.0 Oe ac field oscillating at 1116, 633, 300, and 50 Hz. Diamagnetic corrections were made with Pascal's constants.[21] **CAUTION!** Metal perchlorates containing organic ligands are potentially explosive. Only a small amount of material should be prepared and it should be handled with great care.

Synthetic Procedure. $[CuTb(hmp)_2(NO_3)_3(H_2O)_2]$ (1·Tb). To an aqueous solution (15 mL) of $Cu(NO_3)_2\cdot 3H_2O$ (0.242 g, 1 mmol) was added a solution of Hhmp (0.218 g, 2 mmol). After the mixture was stirred at about 50 °C for 1 h, $Tb(NO_3)_3\cdot 5H_2O$ (0.435 g, 1 mmol) was added. The resulting blue solution was adjusted to pH = 6 with an aqueous NaOH solution (1 M). The filtrate was allowed to slowly evaporate at ambient temperature over 40 days, and then blue polyhedral crystals of **1**·Tb were collected in 66% yield (0.436 g). Elemental analysis calcd for $C_{12}H_{16}CuN_5O_{13}Tb$ (%): C 21.82; H 2.44; N 10.61. Found: C 21.79; H 2.46; N 10.58. Selected IR data ($\tilde{\nu}/cm^{-1}$, KBr pellet): 3502(br), 1608(s), 1466(m), 1356(m), 1217(m), 1165(m), 1075(s), 775(m), 657(m), 585(m), 439(w).

$[Cu_2Tb(mmi)_4(NO_3)(H_2O)_2](ClO_4)(NO_3)\cdot 2H_2O$ (2·Tb). After heating of a mixture of Hmmi (0.109 g, 1 mmol) and $Cu(NO_3)_2\cdot 3H_2O$ (0.242 g, 1 mmol) in distilled water (6 mL) at 60 °C for 10 min, an aqueous solution of $Tb(NO_3)_3\cdot 5H_2O$ (0.435 g, 1 mmol) was added dropwise, followed by an aqueous solution (2 mL) of excess $NaClO_4\cdot H_2O$ (0.702 g, 5 mmol) upon stirring for 20 min. The resulting blue solution was adjusted to pH = 6 and allowed to stand in the air at room temperature for 30 days, yielding sky blue needle crystals (yield: 0.298 g, 58%). Elemental analysis calcd for $C_{20}H_{36}ClCu_2N_{10}O_{18}Tb$ (%): C 23.41; H 3.54; N 13.65. Found: C 23.26; H 3.61; N 13.52. IR data ($\tilde{\nu}/cm^{-1}$, KBr pellet): 3544(m), 3360s(br), 3270(s), 3149(m), 3122(m), 2851(w), 2428(w), 1777-

(8) (a) Osa, S.; Kido, T.; Matsumoto, N.; Re, N.; Pochaba, A.; Mrozinski, J. *J. Am. Chem. Soc.* **2004**, *126*, 420−421. (b) Zaleski, C. M.; Depperman, E. C.; Kampf, J. W.; Kirk M. L.; Pecoraro, V. L. *Angew. Chem., Int. Ed.* **2004**, *43*, 3912−3914.
(9) Costes, J.-P.; Clemente-Juan, J. M.; Dahan, F.; Milon, J. *Inorg. Chem.* **2004**, *43*, 8200−8202.
(10) For recent examples: (a) Sokol, J. J.; Hee, A. G.; Long, J. R. *J. Am. Chem. Soc.* **2002**, *124*, 7656−7657. (b) Choi, H. J.; Sokol J. J.; Long, J. R. *Inorg. Chem.* **2004**, *43*, 1606−1608. (c) Zhuang, Z. J.; Seino, H.; Mizobe, Y.; Hidai, M.; Fujishima, A.; Ohkoshi, S.; Hashimoto, K. *J. Am. Chem. Soc.* **2000**, *122*, 2952−2953. (d) Oshio, H.; Nihei, M.; Yoshida, A.; Nojiri, H.; Nakano, M.; Yamaguchi, A.; Karaki, Y.; Ishimoto, H. *Chem. Eur. J.* **2005**, *11*, 843−848.
(11) (a) Bencini, A.; Benelli, C.; Caneschi, A.; Carlin, R. L.; Dei, A.; Gatteschi, D. *J. Am. Chem. Soc.* **1985**, *107*, 8128−8136. (b) Bencini, A.; Benelli, C.; Caneschi, A.; Dei, A.; Gatteschi, D. *Inorg. Chem.* **1986**, *25*, 572−575.
(12) (a) Costes, J.-P.; Dahan, F.; Dupuis, A.; Laurent, J.-P. *Inorg. Chem.* **1997**, *36*, 3429−3433. (b) Costes, J.-P.; Dahan, F.; Dupuis, A. *Inorg. Chem.* **2000**, *39*, 165−168.
(13) (a) Gheorghe, R.; Andruh, M.; Costes, J.-P.; Donnadieu, B. *Chem. Commun.* **2003**, 2778−2779. (b) Costes, J.-P.; Dahan, F.; Dupuis, A.; Laurent, J.-P. *New J. Chem.* **1998**, 1525−1529. (c) Costes, J.-P.; Dahan, F.; Dupuis, A.; Laurent, J.-P. *Inorg. Chem.* **1996**, *35*, 2400−2402. (d) Koner, R.; Lee, G.-H.; Wang, Y.; Wei, H.-H.; Mohanta, S. *Eur. J. Inorg. Chem.* **2005**, 1500−1505. (e) Shiga, T.; Ohba, M.; Ohkawa, H. *Inorg. Chem.* **2004**, *43*, 4435−4446.
(14) (a) Ryazanov, M.; Nikiforov, V.; Lloret, F.; Julve, M.; Kuzmina, N.; Gleizes, A. *Inorg. Chem.* **2002**, *41*, 1816−1823. (b) Sasaki, M.; Manseki, K.; Horiuchi, H.; Kumahai, M.; Sakamoto, M.; Sakiyama, H.; Nishida, Y.; Sakai, M.; Sadaoka, Y.; Ohba, M.; Okawa, H. *J. Chem. Soc., Dalton Trans.* **2000**, 259−263. (c) Atria, A. M.; Moreno, Y.; Spodine, E.; Garland, M. T.; R.; Baggio. *Inorg. Chim. Acta* **2002**, *335*, 1−6.
(15) (a) Costes, J.-P.; Dahan, F.; Dupuis, A.; Laurent, J.-P. *Inorg. Chem.* **2000**, *39*, 169−173. (b) Costes, J.-P.; Dahan, F.; Dupuis, A. *Inorg. Chem.* **2000**, *39*, 5994−6000. (c) Kou, H.-Z.; Jiang, Y.-B.; Cui, A.-L. *Cryst. Growth Des.* **2005**, *5*, 77−79.
(16) (a) Kahn, M. L.; Mathoniere, C.; Kahn, O. *Inorg. Chem.* **1999**, *38*, 3692−3697. (b) Costes, J.-P.; Dahan, F.; Dupuls, A.; Laurent, J.-P. *Chem. Eur. J.* **1998**, *4*, 1616−1620.
(17) Paulovic, J.; Cimpoesu, F.; Ferbinteanu, M.; Hirao, K. *J. Am. Chem. Soc.* **2004**, *126*, 3321−3331.
(18) (a) He, F.; Tong, M.-L.; Yu, X.-L.; Chen, X.-M. *Inorg. Chem.* **2005**, *44*, 559−565. (b) Yang, Y.-Y.; Huang, Z.-Q.; He, F.; Chen, X.-M.; Ng, S. W. *Z. Anorg. Allg. Chem.* **2004**, *630*, 286−290. (c) Chen, X.-M.; Aubin, S. M. J.; Wu, Y.-L.; Yang, Y.-S.; Mak, T. C. W.; Hendrickson, D. N. *J. Am. Chem. Soc.* **1995**, *117*, 9600−9601.
(19) (a) Chen, X.-M.; Tong, M.-L.; Wu, Y.-L.; Luo, Y.-J. *J. Chem. Soc., Dalton Trans.* **1996**, 2181−2182. (b) Chen, X.-M.; Yang, Y.-Y. *Chin. J. Chem.* **2000**, *18*, 664−672. (c) Yang, Y.-Y.; Ng, S.-W.; Chen, X.-M. *J. Solid State Chem.* **2001**, *161*, 214−224.
(20) Yang, S.-P.; Long, L.-S.; Chen, X.-M.; Ji, L.-N. *Acta Crystallogr., Sect. C* **1999**, *55*, 869−871.
(21) Carlin, R. L. *Magnetochemistry*; Springer-Verlag: Berlin, New York, **1986**.

Table 1. Crystallographic Data and Structure Refinement Parameters for **1**·La, **2**·La, **1**·Gd, **1**·Tb, **2**·Gd, and **2**·Tb

complex	**1**·La	**1**·Gd	**1**·Tb	**2**·La	**2**·Gd	**2**·Tb
chemical formula	$C_{12}H_{16}CuLaN_5O_{13}$	$C_{12}H_{16}CuGd\ N_5O_{13}$	$C_{12}H_{16}CuTb\ N_5O_{13}$	$C_{20}H_{34}ClCu_2LaN_{10}O_{17}$	$C_{20}H_{36}ClCu_2GdN_{10}O_{18}$	$C_{20}H_{36}ClCu_2Tb\ N_{10}O_{18}$
formula weight	640.75	659.09	660.76	988.01	1024.37	1026.04
crystal system	monoclinic	monoclinic	monoclinic	orthorhombic	monoclinic	monoclinic
space group	$P2_1/n$	$P2_1/n$	$P2_1/n$	$P2_12_12_1$	$P2_1/c$	$P2_1/c$
a (Å)	7.5307(6)	7.5471(4)	7.6049(5)	8.0453(7)	8.1322(7)	8.1445(6)
b (Å)	19.9609(15)	19.8537(12)	19.5974(13)	18.6762(16)	18.250(2)	18.2549(13)
c (Å)	14.016(1)	13.8604(8)	13.6724(9)	24.489(2)	24.585(2)	24.6727(18)
β (deg)	105.459(1)	105.220(1)	104.438(1)	90	95.163(2)	97.429(2)
V (Å^3)	2030.7(3)	2004.0(2)	1973.3(2)	3679.6(5)	3633.9(6)	3637.5(5)
Z	4	4	4	4	4	4
ρ_{calcd} (g cm^{-3})	3.201	2.185	2.224	1.783	1.872	1.874
T (K)	298(2)	298(2)	298(2)	298(2)	298(2)	298(2)
λ (MoKα) (Å)	0.71073	0.71073	0.71073	0.71073	0.71073	0.71073
μ (MoKα) (mm^{-1})	3.201	4.42	4.71	2.439	3.12	3.24
$R_1(I > 2\sigma(I))^a$	0.0279	0.0288	0.0293	0.0772	0.0705	0.0481
$wR_2{}^a$	0.0317	0.0845	0.0660	0.1234	0.1448	0.1096

^{a} $R_1 = \sum||F_o| - |F_c||/\sum|F_o|$, $wR_2 = [\sum w(|F_o| - |F_c|)^2/\sum w|F_o|^2]^{1/2}$.

Table 2. Selected Bond Lengths (Å) and Angles (deg) for **1**·La, **1**·Gd, and **1**·Tb

	1·La	**1**·Gd	**1**·Tb		**1**·La	**1**·Gd	**1**·Tb
Ln(1)−O(1)	2.444(2)	2.395(3)	2.325(2)	Ln(1)−O(10)	2.671(2)	2.620(3)	2.551(3)
Ln(1)−O(2)	2.418(2)	2.363(2)	2.298(2)	Ln(1)−O(12)	2.555(2)	2.500(3)	2.426(3)
Ln(1)−O(3)	2.646(2)	2.598(3)	2.547(2)	Ln(1)−O(13)	2.567(3)	2.517(4)	2.441(3)
Ln(1)−O(4)	2.716(2)	2.702(3)	2.585(3)	Cu(1)−O(1)	1.889(2)	1.889(2)	1.887(2)
Ln(1)−O(6)	2.719(2)	2.675(3)	2.810(3)	Cu(1)−O(2)	1.900(2)	1.902(2)	1.896(2)
Ln(1)−O(7)	2.666(2)	2.591(2)	2.491(3)	Cu(1)−N(1)	1.978(2)	1.976(3)	1.972(3)
Ln(1)−O(9)	2.609(2)	2.550(2)	2.476(2)	Cu(1)−N(2)	1.971(2)	1.974(3)	1.971(3)
O(1)−Ln(1)−O(2)	64.23(7)	65.28(8)	66.20(8)	Cu(1)−O(1)−Ln(1)	102.23(8)	102.06(10)	102.14(10)
O(1)−Cu(1)−O(2)	86.03(9)	85.21(11)	83.71(10)	Cu(1)−O(2)−Ln(1)	102.84(8)	102.83(10)	102.85(10)

(w), 1658(m), 1632(m), 1504(s), 1449(s), 1384(s), 1351(s), 1297-(s), 1167(m), 1083(s), 1034(m), 774(m), 592(m), 488(w).

$[CuGd(hmp)_2(NO_3)_3(H_2O)_2]$ (1·Gd). The synthetic method was similar to that for **1**·Tb by using $Gd(NO_3)_3$ instead of $Tb(NO_3)_3$ (Yield: 0.409 g, 62%). Elemental analysis calcd for $C_{12}H_{16}CuGdN_5O_{13}$: C 21.85; H 2.45; N 10.63. Found: C 21.79; H 2.48; N 10.57. Selected IR data ($\tilde{\nu}$/cm^{-1}, KBr pellet): 3503(br), 1608-(s), 1467(m), 1355(m), 1216(m), 1166(m), 1079(m), 774(m), 658-(m), 584(m), 438(w).

$[Cu_2Gd(mmi)_4(NO_3)(H_2O)_2](ClO_4)(NO_3)\cdot 2H_2O$ (2·Gd). The synthetic method was similar to that for **2**·Tb by using $Gd(NO_3)_3$ instead of $Tb(NO_3)_3$ (yield: 0.282 g, 55%). Elemental analysis calcd for $C_{20}H_{36}ClCu_2GdN_{10}O_{18}$ (%): C 23.45; H 3.54; N 13.67. Found: C 23.34; H 3.59; N 13.58. IR data ($\tilde{\nu}$/cm^{-1}, KBr pellet): 3543(m), 3358s(br), 3269(s), 3147(m), 3124 (m), 2858(w), 2422(w), 1778-(w), 1657(m), 1631(m), 1503(s), 1447(s), 1382(s), 1355(s), 1295-(s), 1164(m), 1081(s), 1031(w), 776(m), 594(m), 481(w).

$[CuLa(hmp)_2(NO_3)_3(H_2O)_2]$ (1·La). It was prepared as for **1**·Tb (yield 0.372 g, 58%). Elemental analysis calcd for $C_{12}H_{16}CuLaN_5O_{13}$ (%): C 22.49; H 2.52; N 10.93. Found: C 22.41; H 2.46; N 10.98. Selected IR data ($\tilde{\nu}$/cm^{-1}, KBr pellet): 3498(br), 1604(s), 1464(m), 1355(m), 1216(m), 1167(m), 1077(s), 772(m), 652(m), 583(m), 442(w).

$[Cu_2La(mmi)_4(NO_3)_2(H_2O)](ClO_4)\cdot 2H_2O$ (2·La). It was prepared as for **2**·Tb (yield 0.252 g, 51%). Elemental analysis calcd for $C_{20}H_{34}ClCu_2LaN_{10}O_{17}$ (%): C 24.31; H 3.47; N 14.18. Found: C 24.27; H 3.51; N 14.11. IR data ($\tilde{\nu}$/cm^{-1}, KBr pellet): 3538(m), 3358s(br), 3268(s), 3144(m), 3128(m), 2842(w), 2435(m), 1771-(w), 1653(m), 1636(m), 1503(s), 1445(s), 1388(s), 1354(s), 1292-(s), 1164(m), 1081(s), 1037(m), 771(m), 597(m), 478(w).

X-ray Crystallography. Selected crystallographic data for **1**·Gd, **1**·Tb, **1**·La, **2**·Gd, **2**·Tb and **2**·La are given in Table 1. The data collections were carried out on a Bruker SMART Apex CCD diffractometer using graphite-monochromated MoKα radiation (λ = 0.71073 Å) at 293 K by using frames of 0.3° oscillation ($4.3 \leq 2\theta \leq 60°$). Absorption corrections were applied by using SADABS.[22] The structures were solved with direct methods and refined with a full-matrix least-squares technique with the SHELXTL programs.[23] Anisotropic thermal parameters were applied to all non-hydrogen atoms. The organic hydrogen atoms were generated geometrically (C−H 0.96 Å); the aqua hydrogen atoms were located from difference maps and refined with isotropic temperature factors. Selected bond lengths and bond angles are listed in Tables 2 and 3.

Results and Discussion

Synthesis. Hhmp and Hmmi are O- and N-donors and can be considered bridging ligands with different coordinating abilities. Lanthanide cations are hard acids and extremely oxophilic and, therefore, prefer to interact with the O-donors. Copper(II) ion is a borderline acid, and can bind to both the

(22) Sheldrick, G. M. *Program for Empirical Absorption Correction of Area Detector Data*; University of Göttingen, 1996.
(23) Sheldrick, G. M. *SHELXTL*, Version 6.10; Bruker Analytical X-ray Systems, Madison, WI, 2001.

Table 3. Selected Bond Lengths (Å) and Angles (deg) for **2**·La, **2**·Gd and, **2**·Tb

	2·La	**2**·Gd	**2**·Tb		**2**·La	**2**·Gd	**2**·Tb
Ln(1)−O(1)	2.419(7)	2.303(5)	2.288(4)	Cu(1)−O(1)	1.889(8)	1.910(5)	1.905(4)
Ln(1)−O(2)	2.466(7)	2.355(5)	2.343(3)	Cu(1)−O(2)	1.929(8)	1.933(5)	1.930(4)
Ln(1)−O(3)	2.415(7)	2.308(5)	2.288(3)	Cu(2)−O(3)	1.916(7)	1.911(5)	1.902(4)
Ln(1)−O(4)	2.461(7)	2.363(5)	2.357(3)	Cu(2)−O(4)	1.923(7)	1.933(5)	1.933(4)
Ln(1)−O(5)	2.669(11)	2.440(6)	2.406(4)	Cu(1)−N(1)	1.914(12)	1.949(7)	1.949(5)
Ln(1)−O(6)	2.509(9)	2.358(7)	2.338(4)	Cu(1)−N(2)	1.943(12)	1.937(6)	1.929(5)
Ln(1)−O(7)	2.701(10)	2.606(6)	2.601(5)	Cu(2)−N(3)	1.950(9)	1.944(7)	1.950(5)
Ln(1)−O(8)	2.679(8)	2.493(6)	2.480(4)	Cu(2)−N(4)	1.948(9)	1.927(7)	1.932(5)
O(1)−Ln(1)−O(2)	64.3(3)	67.07(18)	67.06(12)	O(3)−Cu(2)−O(4)	85.4(3)	84.4(2)	83.97(15)
O(3)−Ln(1)−O(4)	64.6(2)	67.10(18)	67.03(12)	Cu(1)−O(2)−Ln(1)	103.2(3)	103.0(2)	103.18(15)
O(1)−Cu(1)−O(2)	85.9(3)	84.1(2)	83.67(15)	Cu(2)−O(3)−Ln(1)	105.9(3)	105.5(2)	106.23(16)
Cu(1)−O(1)−Ln(1)	106.2(3)	105.7(2)	106.05(16)	Cu(2)−O(4)−Ln(1)	103.9(3)	102.8(2)	102.65(15)

N- and O-donors. Based on our previous studies of 3d−4f systems,[19] sodium perchlorate can enhance the crystallization. In fact, all complexes in this work were prepared in better yields with the presence of sodium perchlorate, furnishing a series of dinuclear $Cu^{II}Ln^{III}$ complexes (Ln = La, Gd, or Tb) with the general formula $CuLn(hmp)_2(NO_3)_3(H_2O)_2$ (**1**) and trinuclear $Cu^{II}Ln^{III}Cu^{II}$ complexes (**2**) by one-pot reactions in water.

Description of Crystal Structures. $[CuLn(hmp)_2(NO_3)_3(H_2O)_2]$ (1·Gd, 1·La, and 1·Tb). X-ray structural analysis reveals that **1**·Gd consists of a discrete neutral dinuclear $[CuGd(hmp)_2(NO_3)_3(H_2O)_2]$ molecule (Figure 1), which consists of a pair of Cu^{II} and Gd^{III} ions bridged by two hmp μ-alkoxo groups. The cyclic CuO_2Gd entity is not coplanar, but in a roof-shaped fashion with a dihedral angle of 20.5° between the O(1)−Cu(1)−O(2) and the O(1)−Gd(1)−O(2) planes. The Cu^{II} ion adopts a twisted square coordination geometry with two hmp ligands: Cu−N 1.973(3) and 1.976(3) Å; Cu−O 1.890(3) and 1.900(3) Å. The deviations of these four atoms and the Cu^{II} ion from this N_2O_2 least-squares plane are 0.2299 Å for O(1), −0.2290 Å for O(2), −0.1826 Å for N(1), 0.1817 Å for N(2), and −0.0034 Å for Cu(1). These results indicate that the coordination sphere around the Cu^{II} is largely distorted toward tetrahedral. The Gd^{III} ion is deca-coordinated in a distorted dicapped square-antiprism geometry, which is ligated by a $Cu(hmp)_2$ entity, three nitrate anions, and two water molecules. Besides two bridging oxygen atoms, Gd−O 2.395(3) and 2.364(3) Å, the Gd^{III} ion is further coordinated by six oxygen atoms from three η^2 chelating nitrates, Gd−O 2.547(3) ∼2.705(3) Å, and two aqua ligands, Gd−O 2.506(3) and 2.524(3) Å. The shorter Gd−O bonds involve the hmp ligands and the longer ones involve the nitrates. The intramolecular Cu···Gd distance is 3.345(1) Å, which is within the usual range reported in the literature.[24] Indeed, magnetic interactions can be present between metal ions separated by a large distance through atoms, radicals, or weak interactions such as hydrogen bonding and $\pi-\pi$ stacking. In **1**·Gd, the shortest intermolecular metal−metal separations are large (Cu···Cu 5.44 Å, Gd···Gd 7.01 Å, and Cu···Gd 7.52 Å). They exclude any significant intermolecular magnetic interaction.

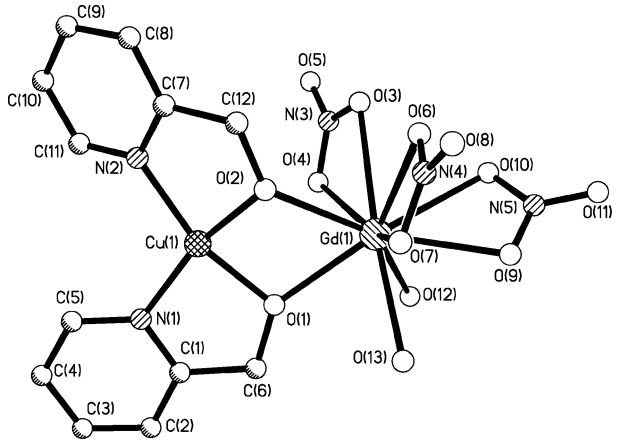

Figure 1. Perspective view of **1**·Gd.

The crystal structures of both **1**·Tb and **1**·La are isomorphous to that of **1**·Gd; hence, only very small metric differences have been observed for these complexes. Because the radii of the three lanthanide ions are in the order of La^{III} > Gd^{III} > Tb^{III}, all the metal−ligand bonds in **1**·Tb are slightly smaller than the corresponding bonds in **1**·Gd, while those of **1**·La are larger, as compared in Table 3. However, the dihedral angle between the O(1)−Cu(1)−O(2) and the O(1)−Tb(1)−O(2) planes is markedly larger in **1**·Tb (21.4°) than in **1**·Gd (20.5°). In **1**·La, the dihedral angle between the O(1)−Cu(1)−O(2) and the O(1)−La(1)−O(2) planes is 20.6°.

$[Cu_2Ln(mmi)_4(NO_3)(H_2O)_2](ClO_4)(NO_3)\cdot 2H_2O$ (2·Gd and 2·Tb). X-ray structural analysis revealed that **2**·Gd and **2**·Tb are isostructural and only minor geometric differences were found. Therefore, only the structure of **2**·Gd is described.

In the trinuclear $[\{Cu(mmi)_2\}_2Gd(NO_3)(H_2O)_2]^{2+}$ core of **2**·Gd, the Gd^{III} center is surrounded by two $Cu(mmi)_2$ entities in which the bond lengths and angles of the two $Cu(mmi)_2Gd/2$ moieties differ only slightly. In addition to the trinuclear entities, the unit cell contains one uncoordinated nitrate ion, one perchlorate ion, and two lattice aqua molecules. A view of the trinuclear cation is represented in Figure 2. The central Gd^{III} is linked to each Cu^{II} ion by four μ-alkoxo bridges from the mmi ligands. The dihedral angles between the O−Cu−O and the O−Gd−O planes are 2.4° and 4.4° for Cu(1) and Cu(2), respectively, and are much more coplanar than that in **1**·Gd. The intramolecular Cu···

(24) (a) Novitchi, G.; Shova, S.; Caneschi, A.; Costes, J.-P.; Gdaniec, M.; Stanica, N. *Dalton Trans.* **2004**, 1194−1200. (b) Akine, S.; Matsumoto, T.; Taniguchi, T.; Nabeshima, T. *Inorg. Chem.* **2005**, *44*, 3270−3274. (c) Myers, B. E.; Berger, L.; Friedberg, S. A. *J. Appl. Phys.* **1969**, *40*, 1149−1151.

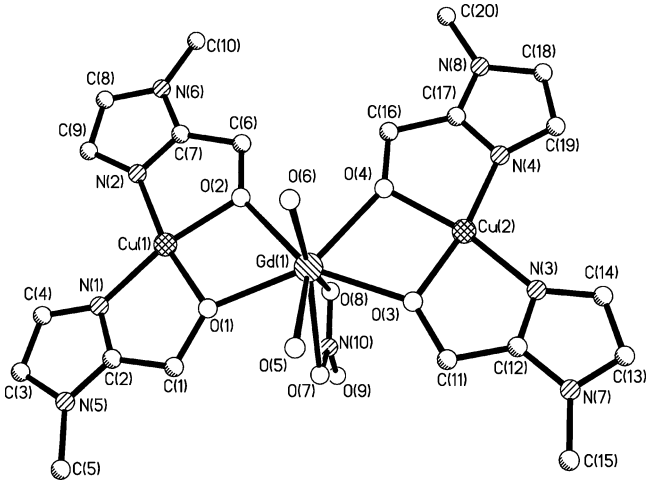

Figure 2. Perspective view of trinuclear cation in **2**·Gd.

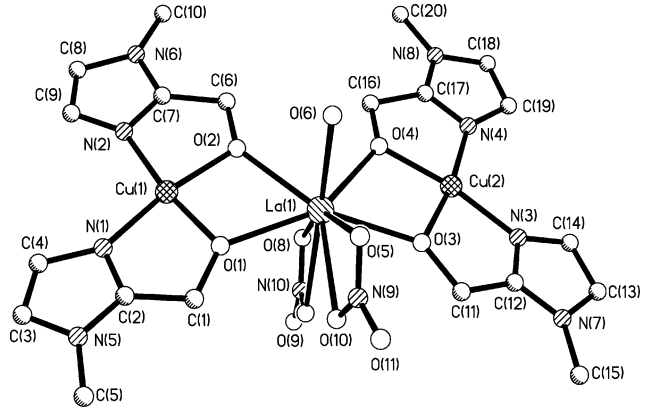

Figure 3. Perspective view of trinuclear cation in **2**·La.

Gd separations (3.367(2) and 3.366(2) Å) in **2**·Gd are slightly longer than those in **1**·Gd (3.345(1) Å).

Each Cu^{II} ion in **2**·Gd has a slightly more planar-square environment (max. deviation from the mean plane 0.0096 Å) compared to that in **1**·Gd. The four basal N_2O_2 donors are afforded by two mmi ligands. The Gd^{III} is eight-coordinated and surrounded by two $Cu(mmi)_2$ fragments (Figure 2). As previously noted, the Gd−O bond lengths depend on the nature of the oxygen atoms, in which the bonds donated by the mmi ligands are shorter (2.303(2)−2.363(5) Å) while the largest one is related to the nitrate ion (2.606(6) Å). In **2**·Gd, a shorter intermolecular Cu···Cu distance (4.988 Å) is found, whereas the intermolecular Gd···Gd and Cu···Gd separations are up to 8.13 and 7.21 Å, respectively. The Cu(1)···Cu(2) distance within the trinuclear entity (6.49 Å) is slightly longer than those of related complexes described in the literature (6.080−6.406 Å).[13b,d,24]

$[Cu_2La(mmi)_4(NO_3)_2(H_2O)](ClO_4)\cdot 2H_2O$ (2·La). A view of the trinuclear cation of **2**·La is depicted in Figure 3. As for **2**·Gd and **2**·Tb, the Cu^{II} atom and its four nearest neighbors (N(1), N(2), O(1), O(2) or N(3), N(4), O(3), and O(4)) form a plane. Interestingly, the crystal of **2**·La belongs to the chiral space group of $P2_12_12_1$ due to the crystal-packing arrangement. Compared with **2**·Gd and **2**·Tb, the La^{III} ion in **2**·La is surrounded by nine oxygen atoms instead of eight and with a nitrate instead of an aqua ligand bound to the La^{III} ion, leading to the different stacking fashion. The occurrence of this additional bidentate nitrate in the La^{III} coordination polyhedron, because of the larger radius of La^{III}, is responsible for a different unit cell which, nevertheless, maintains a structure very similar to those of **2**·Gd and **2**·Tb. The dihedral angles between the O−Cu−O and the O−Gd−O planes are 5.3° and 3.7° for Cu(1) and Cu(2), respectively. The intramolecular Cu···La separations are 3.4611(12) and 3.4689(12) Å. The Cu(1)···Cu(2) distance within the trinuclear entity is 6.65 Å, longer than that in **2**·Gd (6.49 Å).

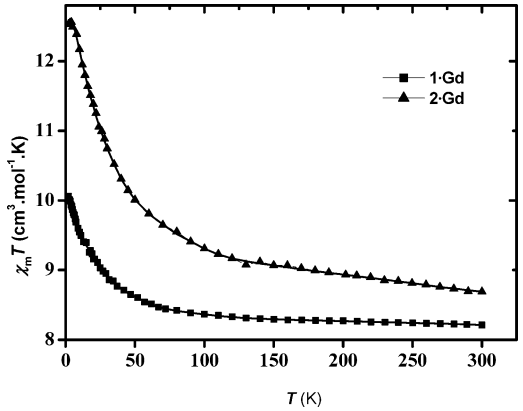

Figure 4. Experimental (squares/triangles) and calculated (solid lines) plots of $\chi_M T$ versus T for **1**·Gd and **2**·Gd.

It is well known that the crystal structures of most of the lanthanide compounds vary along the lanthanide series. In the case of **2**·La with the largest ionic radius, the space group is $P2_12_12_1$ and the Ln^{III} ion is nine-coordinate. In the cases of **2**·Gd and **2**·Tb with smaller ionic radii, the space groups are $P2_1/c$ and the Ln^{III} ions are eight-coordinate.

Magnetic Properties. 1·Gd and 2·Gd. The magnetic behaviors were investigated for both **1**·Gd and **2**·Gd. The temperature dependences of the magnetic properties in the form of the $\chi_M T$ product vs T are illustrated in Figure 4. For **1**·Gd, $\chi_M T = 8.21$ cm^3 K mol^{-1} at room temperature, a value roughly corresponding to two isolated $S = 1/2$ ($\chi_M T = 0.375$) and $S = 7/2$ ($\chi_M T = 7.875$) ions. Lowering the temperature caused an increase of $\chi_M T$, which reached 10.06 cm^3 K mol^{-1} at 2 K. This behavior reveals a ferromagnetic coupling between $S = 1/2$ and $S = 7/2$, with $S = 4$ ground state.

For **2**·Gd, the $\chi_M T$ value is 8.69 cm^3 K mol^{-1} at 300 K, which corresponds to the value expected for two Cu^{II} ($S = 1/2$) and one Gd^{III} ($4f^7$, $J = 7/2$, $L = 0$, $S = 7/2$, $^8S_{7/2}$) noninteracting ions. As the temperature is lowered, the $\chi_M T$ value gradually increases until it reaches a maximum value of 12.56 cm^3 K mol^{-1} at 4 K. This compares well with the value (12.38 cm^3 K mol^{-1}) anticipated for an $S = 9/2$ spin state resulting from ferromagnetic coupling between Cu^{II} and Gd^{III} and assuming $g_{Cu} = g_{Gd} = 2$. The increase of $\chi_M T$ value in the lower temperature region indicates the operation of a ferromagnetic interaction between the Cu^{II} and Gd^{III} ions.

Gd^{III} with an $^8S_{7/2}$ single-ion ground state does not possess a first-order orbital moment.[25] Thus the contributions of the orbital angular momentum and the anisotropic effect do not need to be taken into consideration; the spin-only formalism

(25) Kahn, O. *Molecular Magnetism*; VCH: Weinhem, 1993.

may be applied to the magnetic study of the **1**·Gd (Cu−Gd) and the **2**·Gd (Cu−Gd−Cu) clusters. Considering the occurrence of intramolecular magnetic interactions (J) and intermolecular interactions (J''),[24a,c] the coupling of the spin momentum of Gd^{III} and Cu^{II} ions is described by the spin Hamiltonian $H = -J_{CuGd}S_{Cu}S_{Gd} - J''_{CuCu}S_{Cu}S_{Cu}$. Viewing the g values associated with the low lying levels $E(4) = 0$ and $E(3) = 4J$, $g_4 = (7g_{Gd} + g_{Cu})/8$ and $g_3 = (9g_{Gd} - g_{Cu})/8$, the theoretical expression is as follows

$$F_d = \frac{15g_4^2 + 7g_3^2\, e^{-4J/kT}}{9 + 7\, e^{-4J/kT}} \quad (1)$$

$$\chi T = \frac{4N\beta^2 TF_d}{kT - J''F_d} + N_\alpha T \quad (2)$$

Here β is the Bohr magneton, g is Lande g factor, k is Boltzman's constant, and N_α is the temperature-independent paramagnetism. A least-squares fitting of the experimental data leads to the following set of parameters for **1**·Gd (Figure 4): $g_{Gd} = 1.99(2)$, $g_{Cu} = 2.04(1)$, $J = 3.36(1)$ cm^{-1}, $J'' = -0.018(6)$ cm^{-1}, $N_\alpha = 2.51 \times 10^{-5}$ cm^3 mol^{-1}, and the residue factor $R = 2.1 \times 10^{-5}$. This fitting indicates an intramolecular Cu−Gd ferromagnetic interaction. The observed J value in **1**·Gd is rather similar to those with the magnetic interaction mediated by CuO_2Gd cores.[13b,26]

To keep the occurrence of two types (J_{GdCu}, J'_{CuCu}) of intramolecular magnetic interactions for **2**·Gd, analysis of the magnetic properties for the trinuclear complexes (Cu−Gd−Cu) is based on the Hamiltonian equation $H = -J/2(S^2 - 2S_{Cu} - S^2_{Gd}) - (J' - J)/2(S^2 - 2S^2_{Cu})$. Based on the Van Vleck equation, the magnetic susceptibility expression for this system is obtained.[24a]

$$g_{9/2,1} = \frac{2}{9}g_{Cu} + \frac{7}{9}g_{Gd}, \quad g_{7/2,1} = \frac{4}{63}g_{Cu} + \frac{59}{63}g_{Gd},$$
$$g_{5/2,1} = \frac{-10}{35}g_{Cu} + \frac{45}{35}g_{Gd}, \quad g_{7/2,0} = g_{Gd} \quad (3)$$

$$F_t = \frac{\frac{495}{2}g^2_{9/2,1} + 126g^2_{7/2,1}\, e^{-9J/2kT} + \frac{105}{2}g^2_{5/2,1}\, e^{-8J/kT} + 126g^2_{7/2,0}\, e^{(J'-7/2J)/kT}}{10 + 8\, e^{-9J/2kT} + 6\, e^{-8J/kT} + 8\, e^{(J'-7/2J)/kT}} \quad (4)$$

$$\chi T = \frac{N\beta^2 TF_t}{3kT - J''F_t} + N_\alpha T \quad (5)$$

For **2**·Gd, the least-squares fitting gives the following values: $g_{Gd} = 1.99(1)$, $g_{Cu} = 2.01(2)$, $J = 5.76(2)$ cm^{-1}, $J' = 3.97(1)$ cm^{-1}, $J'' = -0.007(3)$ cm^{-1}, $N_\alpha = 3.76 \times 10^{-5}$ cm^3 mol^{-1}, and the residue factor $R = 2.5 \times 10^{-5}$.

The field dependence of the magnetization for **1**·Gd and **2**·Gd measured at 2.0 K is shown in Figure 5, where M and H are magnetization and applied magnetic field, respectively. The experimental values are well fitted by the Brillouin function for an $S = 4$ spin state, which confirms the ferromagnetic nature of the Cu−Gd interaction. The experimental values for **2**·Gd nicely follow the Brillouin function for an $S = 9/2$ spin state, indicating the ferromagnetic nature of the Cu−Gd−Cu clusters and the absence of Cu−Cu antiferromagnetic interactions in these trinuclear entities, which are similar to the related complexes reported previously.[24] Since the magnetic coupling is dependent on the exchange transfer integral between the 3d orbital of Cu^{II} and the 4f orbital of Gd^{III},[27] a heterometal complex with a more planar bridging moiety should exhibit a stronger ferromagnetic interaction. The comparisons of the structural and magnetic characteristics in the CuO_2Gd bridging network reported in the literature are listed in Table 4. It was noted that the J_{CuGd} values and the dihedral angle α defined by the two O−Cu−O and O−Gd−O planes of the CuO_2Gd bridging entity could be correlated by an exponential function.[12b] Indeed, the reported dihedral angles α are in the range of 1.7−47.4°, and are well fitted to the correlation between the absolute value of the ferromagnetic coupling constant J and the dihedral angle of $|J| = A\exp(B\alpha)$, with $A = 12.49$ and $B = -0.0611$, correlation coefficient $R^2 = 0.9145$ (see Figure 6). This magnetostructural correlation revealed that the increase of the interaction parameter J can be related to a decrease in α and tends to vanish when α

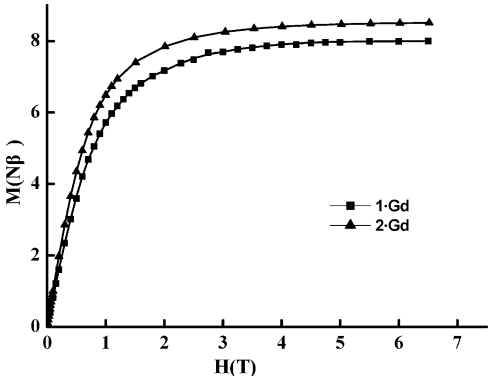

Figure 5. Field dependence of the magnetization for **1**·Gd and **2**·Gd. The solid lines represent the theoretical magnetization curves for the $S_T = 4$ (**1**·Gd) and 9/2 (**2**·Gd) ground state, respectively.

Table 4. Comparative Table between J Values and the Dihedral Angle (α) for Various Cu^{II}−Gd^{III} Complexes with a CuO_2Gd Bridging Core

formula	J (cm^{-1})	dihedral angle (α) (deg)	refs
Cu(salabza)Gd(hfac)$_3$	0.8	47.4	14b
Gd(hfa)$_3$Cu(salen)	0.4	47.1	27
Cu(acacen)Gd(pta)$_3$	1.47	41.4	14a
Gd(hfa)$_3$Cu(salen)(Meim)	1.42	39.6	27
Cu(acacen)Gd(hfa)$_3$	1.25	39	14a
Cu(salen)Gd(pta)$_3$	1.21	33.1	14a
[CuGd(ems)(NO$_3$)$_3$H$_2$O]Cu(ems)	1.878	24.5	14c
LCu(O$_2$COMe)Gd(thd)$_2$	3.5	19.1	13b
LCuGd(NO$_3$)$_3$	4.98	18.9	26
LCu(C$_3$H$_6$O)Gd(NO$_3$)$_3$	4.8	16.7	12a
LCuGd(O$_2$CCF$_3$)$_3$(C$_2$H$_5$OH)$_2$	4.42	13.6	24a
LCuGd(NO$_3$)$_3$·Me$_2$CO	7.0	12.9	13c
LCu(MeOH)Gd(NO$_3$)$_3$	6.8	12.5	12a
[LCuCl$_2$Gd(H$_2$O)$_4$]Cl·2H$_2$O	10.1	1.7	12
CuGd(hmp)$_2$(NO$_3$)$_3$(H$_2$O)$_2$	3.36	20.5	this work

(26) Costes, J.-P.; Dahan, F.; Novitchi, G.; Arion, V.; Shova, S.; Lipkowski, J. *Eur. J. Inorg. Chem.* **2001**, 1530−1537.

(27) Ramade, I.; Kahn, O.; Jeannin, Y.; Robert, F. *Inorg. Chem.* **1997**, *36*, 930−936.

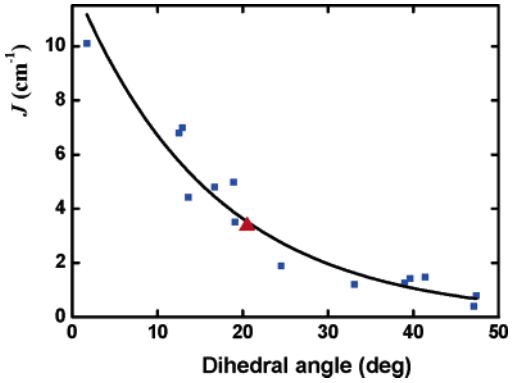

Figure 6. Plots of J versus dihedral angle. The solid line represents theoretical fit for the literature data (■) and 1·Gd (▲) (Table 4).

approaches a value of 47°.[12b] Ferromagnetic interaction observed in **1**·Gd is in agreement with this correlation. It should be noted that the coupling becomes antiferromagnetic for the larger bending values in this series. Based on the literature,[12] it appears that the highest exchange parameters ($J = 10.1$ cm^{-1}) are associated with the lowest value (1.7°). Increasing the α angle to 19.1° and ca. 47.1° causes J to decrease to 3.5 and 0.4 cm^{-1},[27] respectively. In this work, a 3.36 cm^{-1} J value in **1**·Gd is associated with an α angle of 20.5°. The above $|J|-\alpha$ relationship for the dinuclear system cannot be directly applied to **2**·Gd due to the more complicated trinuclear structure. On the other hand, the limited amount of currently known examples of trinuclear Cu_2Gd preclude the possibility of the deduction of a relevant $|J|$-α relationship. However, the bridging CuO_2Gd motifs in **2**·Gd have two different dihedral angles of 2.4° and 4.4°, which may correspond to the two different J values of 5.76-(2) cm^{-1} and 3.97(1) cm^{-1}, respectively. This fact applies to the trinuclear system and there may also be a similar trend found for the dinuclear system.

1·La and 2·La. The magnetic behaviors of **1**·La and **2**·La are shown in Figure S1 (Supporting Information) in the form of $\chi_M T$ versus T. The $\chi_M T$ product for the **1**·La equals 0.376 cm^3 K mol^{-1}. Obviously, this value is equal to the expected value originating only from uncorrelated spins ($S = 1/2$) since no contribution is expected from the nonmagnetic La^{III} ions. For the **2**·La, the room temperature value of $\chi_M T$ is 0.77 cm^3 K mol^{-1}, a value close to that expected for two noninteracting Cu^{II} ions. The data over the whole temperature range 2−300 K are well fitted to the Curie law with $C = 0.79$ cm^3 K mol^{-1}; such behavior indicates no significant Cu−Cu interaction through the 4f ion. Therefore, in the case of **2**·Gd, the coupling of two Cu^{II} ions has been neglected for the sake of simplicity.

1·Tb and 2·Tb. As depicted in Figure 7, the $\chi_M T$ value of **1**·Tb is ca. 12.08 cm^3 K mol^{-1} at room temperature, close to the expected value of 12.19 cm^3 K mol^{-1} for one noninteracting Tb^{III} (4f^8, $J = 6$, $S = 3$, $L = 3$, $^7F_6$) ion and one Cu^{II} ($S = 1/2$) ion. The $\chi_M T$ value of **1**·Tb decreases slightly from 12.08 cm^3 K mol^{-1} at 300 K to 11.92 cm^3 K mol^{-1} at 120 K, whereupon the $\chi_M T$ value decreases significantly to ca. 16 K, and then decreases rapidly. In contrast, upon lowering the temperature, the $\chi_M T$ value of **2**·Tb gradually increases from 12.54 cm^3 K mol^{-1} at 300 K,

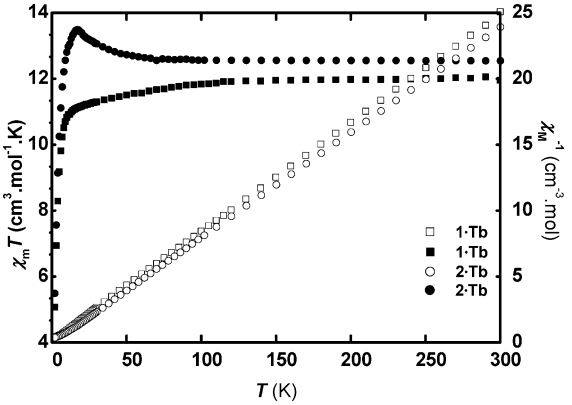

Figure 7. Plots of $\chi_M T$ versus T and $1/\chi_M$ versus T for **1**·Tb and **2**·Tb.

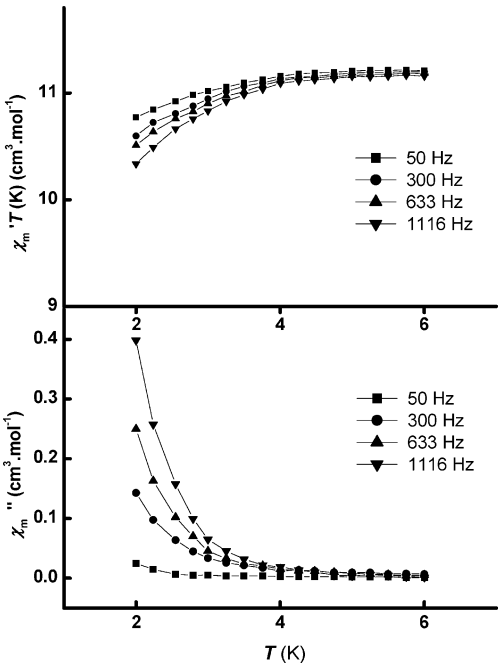

Figure 8. Plots of $\chi'_M T$ vs T (top) and χ''_M vs T for **1**·Tb in a 3.0 G ac field oscillating at the indicated frequencies (and without applied dc field).

which corresponds to the expected value for two isolated Cu^{II} and one Tb^{III} ions, and reaches a maximum value of 13.49 cm^3 K mol^{-1} at 17 K. Upon lowering the temperature further, $\chi_M T$ decreases abruptly to 5.49 cm^3 K mol^{-1} at 2 K. The increase of the $\chi_M T$ value at the lower temperatures indicates a ferromagnetic interaction between the Cu^{II} and Tb^{III} ions.

The ac measurements were carried out in a 3.0 G ac field oscillating at the indicated frequencies and with a zero dc field. In the range 4−30 K, the value of $\chi_M' T$ (χ_M' is the in-phase ac susceptibility) for **1**·Tb is constant at 12.7 cm^3 K mol^{-1}. Below 4.0 K, the in-phase ac susceptibility ($\chi_M' T$) signal begins to decreases (Figure 8a), suggesting that at these temperatures the magnetization of **1**·Tb cannot reverse its direction fast enough to keep in phase with the oscillating ac field. This observation was confirmed by the concomitant appearance of an out-of-phase signal (χ_M'') which exhibits frequency-dependent behavior (Figure 8b). This behavior is indicative of the slow relaxation of the magnetization, which is similar to those found for some lanthanide paramagnetic

ions[28a] without an applied field. Slow relaxation of the magnetization is directly responsible for this behavior in SMM,[1] SCM,[28b] superparamagnetic,[29] or spin-glass[30] systems. Unfortunately, due to the 2 K temperature limit of the instrument, a maximum in the χ_M'' signal was not observed at frequencies as high as 1116 Hz and we did not observe hysteretic behavior in the magnetization of **1**·Tb. On the other hand, the frequency dependence for **2**·Tb is not obvious.

In fact, aside from the difference in the nuclearity, the structural data reveal that the most pertinent difference between **1**·Tb and **2**·Tb exists in the cyclic CuO_2Tb entities, which are bent and coplanar. In **1**·Tb, the dihedral angle is 21.4°, while in **2**·Tb, the dihedral angles are 1.8° and 3.3°. Similar to the trend found for the dinuclear CuGd complexes **2**·Tb exhibits an apparent ferromagnetic interaction for the significantly smaller dihedral angles, compared to that of **1**·Tb with a larger dihedral angle (Figure 7). On the other hand, the frequency dependence for **1**·Tb is more obvious than that of **2**·Tb. Presumably, the geometry of such cyclic CuO_2Tb entity may play an important role in tuning the magnetic properties of the complexes.

Conclusion

We have developed facile one-pot reactions to generate the dinuclear and trinuclear 3d−4f complexes, which exhibit different magnetic properties. Dinuclear **1**·Tb presents the smallest magnetic units in the 3d−4f heterometallic systems that exhibit frequency-dependent behaviors. In the Cu^{II}-Gd^{III} system, it appears that the decrease of the interaction parameter *J* can be related to an increase in the dihedral angle α defined by the two OCuO and OGdO planes of the bridging network.

Acknowledgment. This work was supported by the National Natural Science Foundation of China (no. 20131020) and the Scientific and Technological Bureau of Guangdong Province (no. 04205405).

Supporting Information Available: X-ray crystallographic file in CIF format and additional plots for Figure S1 in PDF. This material is available free of charge via the Internet at http://pubs.acs.org.

IC0507159

(28) (a) Barbara, B.; Giraud, R.; Wernsdorfer, W.; Mailly, D.; Lejay, P.; Tkachuk, A.; Suzuki, H. *J. Magn. Magn. Mater.* **2004**, *272*−*276*, 1024−1029. (b) Clérac, R.; Miyasaka, H.; Yamashita, M.; Coulon, C. *J. Am. Chem. Soc.* **2002**, *124*, 12837−12844.

(29) Oshio, H.; Hoshino, N.; Ito T. *J. Am. Chem. Soc.* **2000**, *122*, 12602−12603.

(30) Buschmann W. E.; Miller J. S. *Inorg. Chem.* **2000**, *39*, 2411−2421.